Tumor Regression *In Vivo* by Photothermal Therapy Based on Gold-Nanorod-Loaded, Functional Nanocarriers

Won Il Choi,[†] Ja-Young Kim,[†] Chul Kang,[‡] Clare C. Byeon,[§] Young Ha Kim,[†] and Giyoong Tae[†,*]

[†]School of Materials Science and Engineering and Department of Nanobio Materials and Electronics, and [‡]Nanophotonic Laboratory, Advanced Photonics Research Institute, Gwangju Institute of Science and Technology, 261 Cheomdan-gwagiro, Buk-gu, Gwangju 500-712, Korea, and [§]School of Mechanical Engineering, Kyungpook National University, 1370 Sangyuk-dong, Buk-gu, Daegu 702-701, Korea

ABSTRACT We developed a very effective hyperthermia system for successful photothermal cancer therapy. Instead of applying individual gold nanorods (GNRs) that can absorb NIR light, GNRs were loaded into functional nanocarriers that could provide stable storage of GNRs and selective delivery to a target tumor site. The functional nanocarriers (chitosan-conjugated, Pluronic-based nanocarriers) were prepared by chemically cross-linking Pluronic F 68 with chitosan conjugation to form a flexible, soft, and excellent reservoir for biomacromolecules as well as tumor targeting. *In vivo* characteristics of the nanocarriers including a long circulation time, a good tumor accumulation, and low liver uptake were previously characterized by us. When GNRs were delivered by using these nanocarriers, much enhanced *in vitro* cellular uptake and a photothermal effect were observed for a cancer cell line. More importantly, an intravenous injection of this system followed by NIR laser irradiation to the tumor site resulted in a very efficient thermolysis *in vivo*. Thus, apparently complete tumor resorption was achieved without damage to the surrounding tissue, suggesting a promising candidate for clinical phototherapeutic applications.

KEYWORDS: Pluronic · nanocarriers · gold nanorods · NIR · photothermal

Photothermal therapy (also referred to as photothermal ablation, photothermolysis, or optical hyperthermia) of solid tumors is an attractive method for treating solid tumors in a minimally invasive manner.[1−6] This technique, which typically involves the conversion of absorbed light into local heating through nonradiative mechanisms, is relatively simple to use for cancer cell ablation and may have several advantages, such as fast recovery, fewer complications, and shorter hospital stay.[7] In particular, the near-infrared (NIR) light used in this manner provides deep-tissue penetration with high spatial precision without damaging normal biological tissues due to the low-energy absorption of NIR light by normal tissues.[8−10]

Several nanostructures, including aggregated gold nanoparticles,[11,12] gold nanoshells,[13−15] gold nanocages,[16] hollow AuAg dendrites,[7] gold nanorods (GNRs),[17−19] carbon nanotubes,[20] and copper sulfide (CuS) nanoparticles,[21] have been investigated for NIR photoactivated cancer therapy. In all cases, light is converted into heat by surface plasmon resonance. In the case of spherical gold nanoparticles, the absorption maximum exists between 400 and 600 nm. Therefore, in *in vivo* applications, very low light penetration and thus inefficient photothermal heating is generated.[12] In contrast, GNRs have attracted much interest because the absorption range of light can be finely tuned by adjusting the aspect ratio, so the heating efficiency can be maximized by using ~800 nm absorption maximum. Also, they have the advantages of efficient large-scale synthesis, easy functionalization, and colloidal stability.[22,23] Despite these advantages, the clinical application of GNRs might be limited due to a slight cytotoxicity caused by the remaining excess cetyltrimethylammonium bromide (CTAB), which is used as a template during synthesis and envelops the surfaces of the GNRs.[19,24] Thus, the surface modifications of GNRs have been reported to reduce the cytotoxic effect;[25] for example, phosphatidylcholine (PC)-modified nanorods,[26] poly(4-styrenesulfonic acid) (PSS)-coated nanorods,[27] GNR-embedded polymeric nanoparticles,[28] and PEG-modified nanorods[29,30] have shown cytotoxicities lower than that of the CTAB-capped nanorods themselves and good photothermal effect.[30]

In addition, specific targeting of GNRs to a target tumor is another key issue for efficient photothermal cancer therapy. Aptamer-conjugated nanorods,[31] folate-conjugated nanorods,[32] and RGD-conjugated dendrimer-modified nanorods[33] have demonstrated

* Address correspondence to gytae@gist.ac.kr.

Received for review November 10, 2010 and accepted February 11, 2011.

Published online February 23, 2011
10.1021/nn103047r

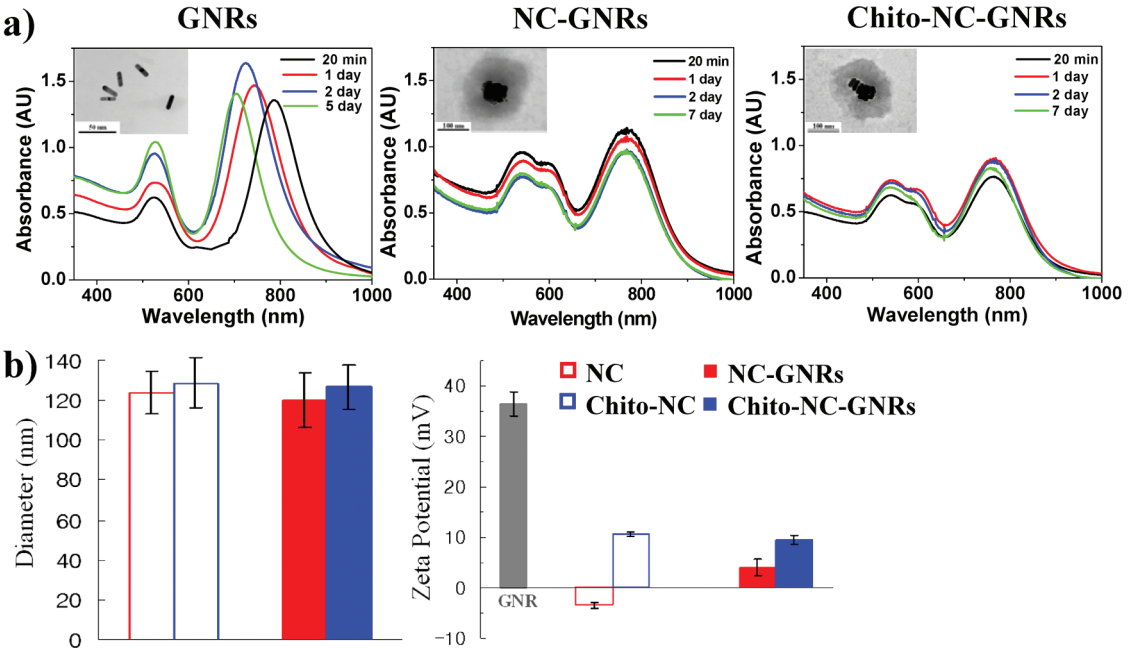

Figure 1. (a) Absorption spectra and transmission electron microscope (TEM) images (inset scale bar = 50 nm in the case of GNRs and 100 nm in the case of other groups) of GNRs themselves and GNR-loaded nanocarriers. (b) Hydrodynamic diameters and surface charges (zeta-potential) of nanocarriers themselves and GNR-loaded nanocarriers (mean ± SD, *n* = 3).

selective and efficient photothermal killing of targeted tumor cells. Although ligand-conjugated GNRs have been effective for photothermal killing of cancer cells *in vitro*, desirable photothermal therapeutic effects in an *in vivo* animal model have been limited due to a high liver uptake during circulation.[34] A high-level localization in the liver of CTAB-stabilized GNRs at 0.5 h after intravenous injection, which might be associated with the hard and rigid characteristics of GNRs, was reported.[29] To overcome the limited effect of GNRs on *in vivo* photothermal cancer therapy, PEGylation of GNRs was attempted to lower the cytotoxicity and the liver accumulation of GNRs.[29] However, complete suppression of tumor growth when using a hyperthermia-based treatment was not achieved, probably due to the very fast excretion of the PEGylated GNRs from the body (half-life of ~1 h). Thus, a new biocompatible vehicle for the efficient delivery of GNRs into tumor sites is still an unmet need for safe and effective cancer therapy based on GNRs.

Previously, we developed photo-cross-linked, Pluronic-based, temperature-sensitive nanocarriers that possessed excellent reservoir characteristics and a simple loading method with high loading capacity for large molecules (*e.g.*, proteins and gold nanoparticles).[35] Importantly, these nanocarriers showed a long circulation time, a good tumor accumulation, and low liver uptake, which were associated with the flexible and soft characteristics as well as the hydrophilic surface from the PEG part of Pluronic. Furthermore, the tumor targeting and prolonged circulation (up to 72 h) were significantly improved and could be optimized by chitosan conjugation (Figure S1 in Supporting Information).[36] Therefore, in this study, we applied the GNR-loaded, Pluronic-based nanocarriers as a hyperthermia agent for enhanced photothermal cancer therapy. The GNR-loaded nanocarriers showed serum stability and photothermolysis of cancer cells *in vitro*. The GNR concentration and the laser power density required for photodestruction of cancer cells were also significantly reduced, compared to other formulations, by using the nanocarrier system.[31,32] Most of all, the optimized GNR-loaded nanocarriers resulted in a very impressive therapeutic effect *in vivo* in nude mice bearing tumors; an apparently complete resorption of the tumor was achieved.

RESULTS AND DISCUSSION

GNRs are known to have two absorption bands; one is a weak short-wavelength band around 520 nm due to transverse electronic oscillations, and the other is the longitudinal plasmon band, which can be varied from the visible to the NIR region by increasing the aspect ratio (length/width) of GNRs.[37] For effective cancer cell imaging and photothermal cancer therapy,[38] GNRs (aspect ratio of ~4) with a longitudinal absorption band at around 800 nm were synthesized by using the seed-mediated growth method with CTAB templates (Figure 1a).[39] Then, both the bare form made of Pluronic F 68 (NC(PF 68)) and the chitosan-conjugated form (Chito-NC(PF 68)) of Pluronic-based nanocarriers were prepared as carriers for GNRs by using photopolymerization, as previously reported by us (Figure 2).[36] Because they showed excellent reservoir characteristics with a high loading capacity of target molecules as well as the flexible and soft characteristics,

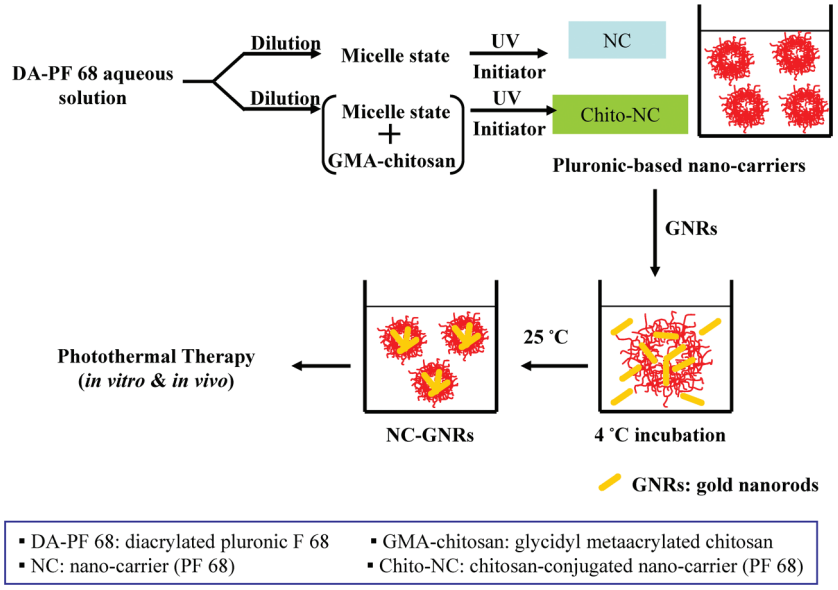

Figure 2. Schematic illustration of the preparation of the Pluronic-based nanocarriers and GNR loading into the nanocarriers.

GNRs with an NIR optical window could be efficiently loaded into the nanocarriers by using co-incubation at 4 °C based on the thermosensitive properties of the nanocarriers, as schematically illustrated in Figure 2.

The morphologies of the GNRs and the GNR-loaded nanocarriers were imaged after negative staining with phosphotungstic acid by using a TEM (insets of Figure 1a). The GNRs were properly loaded inside the nanocarriers for both types without changing the spherical shapes of the nanocarriers. The hydrodynamic diameters and the surface charges (zeta-potential) of the nanocarriers at 37 °C were not affected by the loading of GNRs. As shown in Figure 1b, the nanocarriers themselves and the GNR-loaded nanocarriers had similar average sizes. While the zeta-potentials of the GNRs stabilized in a CTAB solution showed a highly positively charged surface state (+36.5 ± 2.4 mV), the GNR-loaded nanocarriers showed surface charges similar to that of the nanocarriers themselves, suggesting effective shielding of the GNRs by loading them inside the nanocarriers.

The optical stabilities of the GNRs and the GNR-loaded nanocarriers dispersed in an aqueous solution were also examined at several time points (Figure 1a). The GNRs themselves showed a blue shift (shorter wavelength) of the absorption spectrum, which was previously reported due to the reshaping of the GNRs in an aqueous environment,[40,41] that would limit the use of GNRs in an aqueous environment as initially planned. On the other hand, the GNRs loaded in the nanocarriers resulted in no change in the absorption spectra, not even at day 7, revealing that loading GNRs into nanocarriers could prevent the unstable reshaping of GNRs, presumably by the interaction of GNRs with the nanocarriers.[41] In the presence of serum proteins, the advantage of using the nanocarrier became even

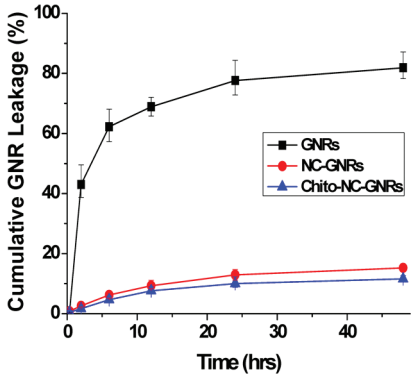

Figure 3. Stable storage of GNRs in the nanocarriers in PBS (pH 7.4, 10% FBS) at 100 rpm and 37 °C.

clearer. GNRs were aggregated and settled down within 1 day, whereas a stable suspension of GNR-loaded nanocarriers with the same absorption spectra was observed. In addition, the nanocarriers could effectively hold the GNRs inside (over 85% in 2 days in the physiological environment, Figure 3). Therefore, the nanocarriers were excellent vehicles for the stable loading of GNRs for further applications.

The cytotoxicity of the GNR-loaded nanocarriers was evaluated by using squamous carcinoma (SCC7) tumor cells and NIH/3T3 fibroblast cells and by using a WST-1 assay. Neither the GNRs nor the GNR-loaded nanocarriers affected the metabolic activities of the two types of cells up to 100 μg/mL (based on GNR amounts), whereas the GNRs themselves showed a much lower cell viability than that of the GNR-loaded nanocarriers at higher concentrations of GNRs in the two types of cells (Figure S2 in Supporting Information). Both types of the nanocarriers themselves showed nearly 100% cell viability up to 1000 μg/mL in the two types of cells, and they were stably dispersed in serum-containing medium without aggregation, as previously reported.[35]

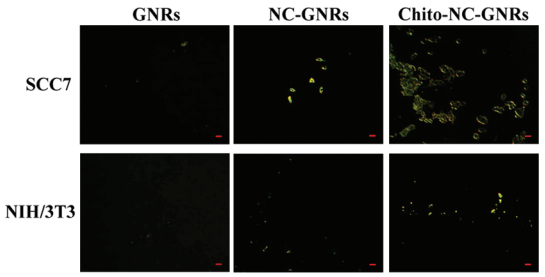

Figure 4. Light scattering images of cells observed by using a dark-field microscope after applying GNRs or GNR-loaded nanocarriers. The scale bar is 10 μm.

Therefore, the nanocarriers used in this study should not cause any acute cytotoxic effect or aggregation during circulation in *in vivo* applications.

The cellular uptake of GNRs was characterized by taking light scattering images (50 μg/mL in terms of GNR amount, Figure 4). The cellular uptake of GNRs was significantly enhanced by loading the GNRs into the nanocarriers. Compared to almost no signal in the case of the direct application of GNRs, the bright spots coming from the GNRs were detected in the cytoplasm, and for the same nanocarriers, a higher cellular uptake was observed from the tumor cells than from normal fibroblast cells, suggesting more efficient cellular uptake of GNRs into tumor cells than normal cells. In addition, the cellular uptake of GNRs was higher for the chitosan-conjugated nanocarriers than the bare nanocarriers. The cellular uptake of the nanocarriers themselves, characterized by using Cy5.5-labeled nanocarriers, also showed results similar to those in the light-scattering images (Figure S3 in Supporting Information).[36] Inefficient cellular uptake by the direct application of GNRs that are covered by CTAB was a good agreement with the previous report.[19] The extent of cellular uptake of chitosan-conjugated nanocarriers was much higher than that of corresponding bare nanocarriers at each incubation time. The enhanced cellular uptake due to chitosan modification has been reported by other systems,[42,43] which might be achieved by several endocytotic pathways as reported for other chitosan-conjugated nanoparticles.[44,45] The characteristic cellular uptake is one of the key factors in *in vivo* tumor targeting because, if nanovehicles are not taken up by the tumor cells, the vehicles will easily diffuse back into the main bloodstream without accumulation. Therefore, the result of an enhanced cellular uptake of GNRs by loading them into nanocarriers, especially chitosan-functionalized nanocarriers, suggests that the GNR-loaded nanocarriers may show more efficient internalization and retention in tumor tissues *in vivo*.

Thus, the GNR-loaded nanocarriers with good biocompatibility and improved cellular uptake may act as an effective photothermal absorber for destroying cancer cells by NIR laser irradiation. GNRs or GNR-loaded nanocarriers (50 μg/mL in terms of GNR amount) were applied to both tumor and fibroblast cells, which were then exposed to laser irradiation at a wavelength of 780 nm with different power densities (41.5 and 26.4 W/cm^2) for 4 min. The cells were then stained with acridine orange and propidium iodide to characterize cell viability. As shown in Figure 5, (1) the photothermolysis effect obtained by using the GNR-loaded nanocarriers was enhanced compared to that obtained by direct application of GNRs, which resulted in almost no cell death; (2) the GNR-loaded nanocarriers had a much better photothermal effect on the cancer cells (SCC7) than on the normal cells (NIH/3T3); and (3) the chitosan-conjugated nanocarriers showed much stronger photothermolysis than the bare nanocarriers. All of these results are in good agreement with the cellular uptake results, as expected. In addition, the higher laser intensity resulted in better results. The region of dead cells (shown in red) was the location of the laser spot, whereas the live cells shown in green were outside the laser spot, indicating that neither the GNR-loaded nanocarriers themselves nor the laser irradiation were cytotoxic, but the cytotoxic effect resulted from photothermal heating. By reducing the laser power density, the photothermal effect was decreased and was not even detectable in the case of fibroblast cells. This *in vitro* result suggests that selective killing of cancer cells is possible in a proper laser intensity range by using chitosan-conjugated nanocarriers as a delivery vehicle for GNRs.

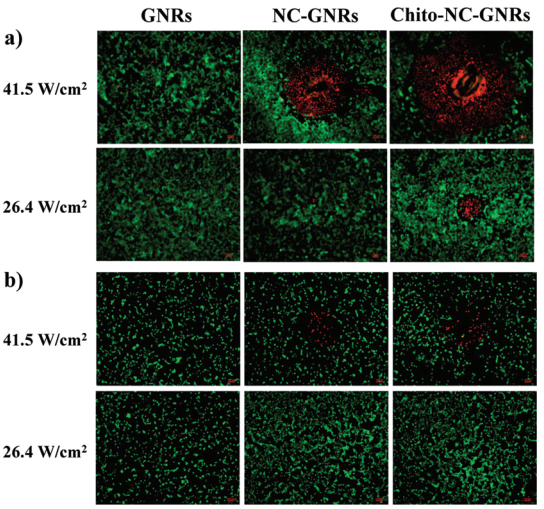

Figure 5. Fluorescence images after selective NIR photothermal therapy on (a) SCC7 cancer cells and (b) NIH/3T3 fibroblast cells with GNRs or GNR-loaded nanocarriers irradiated by a laser at 780 nm with two different power densities (41.5 and 26.4 W/cm^2) for 4 min. Cells were stained with acridine orange (live: green) and propidium iodide (dead: red) after laser irradiation. Scale bar: 100 μm.

To further investigate the photothermal therapeutic effect on cancer cells in an *in vivo* animal model with solid tumors, the GNR-loaded nanocarriers were intravenously (i.v.) injected through the tail vein into

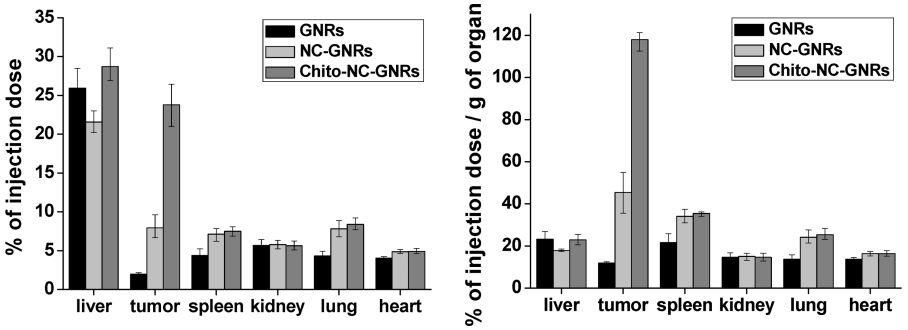

Figure 6. Biodistribution of GNRs or GNR-loaded nanocarriers in nude mice at 24 h after intravenous (tail vein) injection. The gold amounts in tissue samples were measured by ICP-AES (n = 3).

athymic nude mice bearing bilateral SCC7 tumors. Major organs including tumors were excised at 24 h after the i.v. injection to assess the biodistribution of GNRs. Inductively coupled plasma atomic emission spectrometer (ICP-AES) was used to analyze quantitatively the amounts of GNRs in organs and tumors. As shown in Figure 6, GNRs could be more efficiently accumulated into the tumor site by using the nanocarriers than that of GNRs themselves, especially in the case of chitosan-conjugated nanocarriers, which showed over 20% accumulation in tumor. In the case of PEG-modified GNRs, tumor uptake was limited to ~7%, which might result from nonspecific targeting.[30] Figure S4 (in Supporting Information) also shows the silver-staining images of representative areas of tumors and livers from the mice treated with GNR samples or with a saline solution as a negative control. The GNR-loaded chitosan-conjugated nanocarriers showed significantly higher intensities (darker color) at tumor tissues than other groups, revealing more efficient tumor targeting, whereas the strongest intensity in the liver was obtained from the direct application of GNRs, revealing the high liver uptake of the GNRs themselves.

To analyze the therapeutic effect of the GNR-loaded nanocarriers on photothermal ablation of solid tumors, the mice were exposed to NIR laser irradiation (808 nm, 4 W/cm^2) for 4 min at 24 h after the i.v. injection (left tumors: no laser irradiation *vs* right tumors: laser irradiation). As shown in Figure 7, the GNR-loaded nanocarriers resulted in a significant suppression of tumor growth, whereas the direct application of GNRs showed no statistical difference in tumor regression compared to that of the saline-treated group. As expected, the chitosan-conjugated nanocarriers showed remarkably suppressed tumor growth compared to the bare form; no growth in tumor volume was observed for 1 week, and a slow increase was observed after that for one-time laser irradiation, which clearly showed the effective tumor accumulation of chitosan-conjugated nanocarriers and, thus, a very efficient photothermal effect.

We further challenged photothermal cancer therapy with an additional test using two irradiations with the NIR laser for 4 min, one at 24 h and the other at 48 h after the i.v. injection of the GNR-loaded nanocarriers. With one more laser irradiation at day 2, the suppression of tumor growth was improved when using the nanocarriers and was especially more effective for the chitosan-conjugated form, whereas the insufficient suppression of tumor growth in the case of direct application of GNRs (Figure 7c,d) was not changed significantly (no statistical difference). Interestingly, an apparently complete resorption of tumors was observed within 6 days after photothermal therapy in the case of the chitosan-conjugated form (Chito-NC(PF 68)) (see the magnified view of Figure 7c at early time points). This result suggests that a preferential accumulation of the GNR-loaded, chitosan-conjugated nanocarriers was sufficient to achieve a therapeutic level of loaded GNRs in solid tumors for photothermal therapy using an NIR laser without apparently damaging the surrounding healthy tissues.

In a separate *in vitro* experiment, based on the amount of gold in the tumor site (Figure 6), the temperature changes of aqueous buffer containing GNRs and GNR-loaded nanocarriers after laser irradiation for 4 min were analyzed. As expected, the highest temperature increase (47 °C) was observed in the case of Chito-NC-GNRs due to the larger amount of GNRs, whereas 36 and 41 °C were observed in the case of GNRs and NC-GNRs, respectively. However, since this assay was done in the buffer, the actual temperature increase by photothermal therapy in the tumor, which has a larger heat capacity than the buffer solution, would be lower than that. Also, the absorption spectrum of GNR-loaded nanocarriers was not changed after the same light exposure used in the *in vivo* experiment, implying that the therapeutic effect observed in the *in vivo* experiments was dominated by the thermal heating of GNRs by light absorption, not by other factors such as deformation of GNRs into cytotoxic gold nanoparticles after the laser exposure.[46] The minimal amount of GNRs loaded in the nanocarriers that can cause sufficient heating (over 40 °C) by laser irradiation was estimated to be 2.5 μg in 100 mm^3 tumor. In other reports, heating effects were also reported with the similar concentration range of GNRs

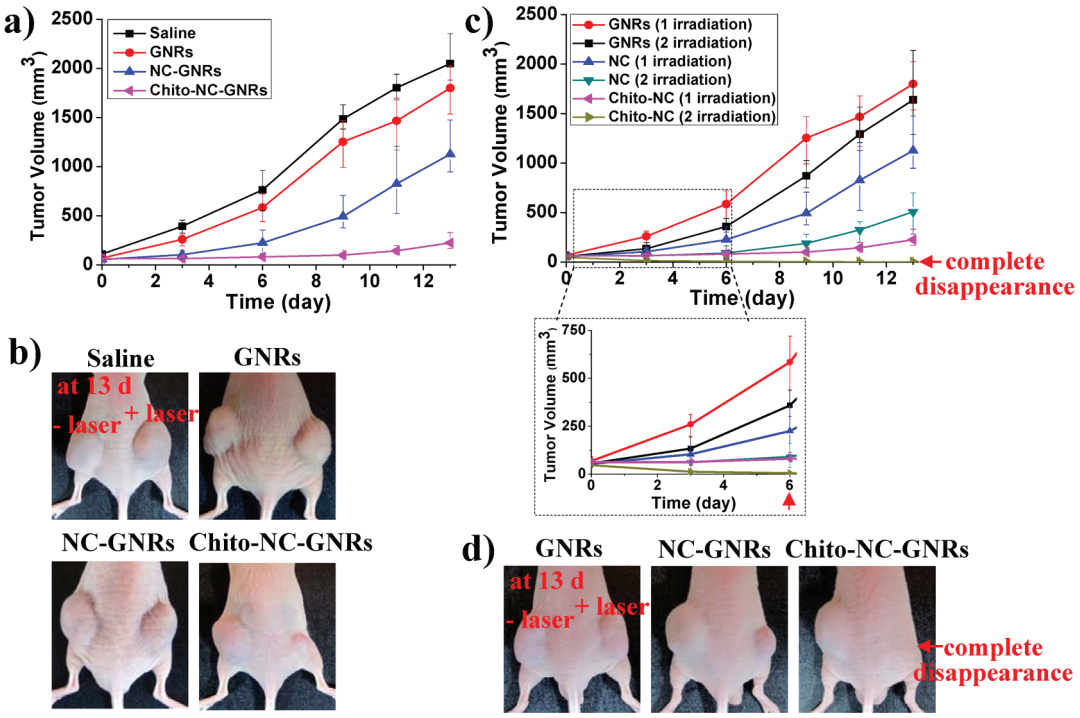

Figure 7. (a) Changes in tumor volumes and (b) the tumor images after onetime NIR laser irradiation (808 nm, 4 W/cm^2) for 4 min at 24 h after the i.v. injection of the nanomaterials. (c) Change in tumor volumes (an enlarged graph at initial time) and (d) the tumor images after NIR laser irradiations at 24 and 48 h after single i.v. injection of the nanomaterials.

by an NIR laser irradiation (11.8 μg/mL for GNR-embedded polymeric nanoparticles[28] and 7 μg/mL for PEG-coated GNRs[30]).

Overall, GNR-loaded Pluronic-based nanocarriers may function as an effective photothermal agent for improved photothermal cancer therapy by the efficient localization of GNRs in tumor. Especially, the use of chitosan-conjugated nanocarriers had a very efficient therapeutic effect on the photothermal ablation of solid tumors *in vivo*. This result corresponds well with our previous report of tumor targeting of the Pluronic-based nanocarriers themselves,[36] which indicates that the tumor-targeting characteristics of the nanocarriers are not changed by loading macromolecules inside them.

In this work, the GNR concentration (50 μg/mL) and the laser intensity (41.5 W/cm^2) required for efficient cancer cell photodestruction *in vitro* were significantly lower than those for other formulations.[31,32,47] In the case of aptamer-conjugated nanorods, GNRs with 85 μg/mL were used on cancer cells and were irradiated at 76 W/cm^2 for selective and effective photothermal therapy *in vitro*. Also, CTAB-capped nanorods (147 or 176 W/cm^2) and antibody-conjugated nanorods (51 W/cm^2) required a higher laser intensity to be more susceptible to hyperthermic effects. In the case of *in vivo* experiment, moderate amounts of GNRs loaded inside the chitosan-conjugated nanocarriers were delivered to the tumor site and resulted in an impressive photothermal therapeutic effect, whereas the PEG-modified GNRs and CTAB-stabilized GNRs were inefficient for tumor targeting, showing very fast excretion or dominant accumulation in the liver,[48] implying an inefficient photothermal effect at the tumor site.

CONCLUSIONS

In conclusion, GNR-loaded, chitosan-conjugated, Pluronic-based nanocarriers were successfully prepared and could serve as imaging agents for cancer cells and as a very effective hyperthermia agent for photothermal cancer therapy with NIR light exposure. Even an apparently complete resorption of tumors *in vivo* was achieved with no damage to the surrounding tissue. These results suggest that the present system has a sufficient tumor-targeting efficiency and is highly effective and safe for transducing NIR light into localized heat; thus, it is a promising candidate for clinical phototherapeutic applications.

EXPERIMENTAL SECTION

Materials. Hydrogen tetrachloroaurate(III) hydrate ($HAuCl_4$) was purchased from Kojima Chemicals Co., Ltd. (Kashiwabara, Japan). Cetyltrimethylammonium bromide (CTAB), sodium borohydride ($NaBH_4$), L-ascorbic acid, glycidyl methacrylate (GMA), sodium chloride, potassium phosphate monobasic, sodium phosphate dibasic, phosphotungstic acid, sodium azide, acridine orange (AO), and propidium iodide (PI) were

obtained from Sigma-Aldrich Corp. (St. Louis, MO). Pluronic F 68 (PF 68) was a kind donation from BASF Corp. (Seoul, Korea). 4-(2-Hydroxyethoxy)phenyl-(2-hydroxy-2-propyl)ketone (Irgacure 2959) was obtained from Ciba Specialty Chemicals Inc. (Basel, Switzerland). Water-soluble chitosan [chitooligosaccharide, molecular weight of *ca.* 10 kDa, deacetylation degree = 85.0%] was purchased from Kittolife Co., Ltd. (Seoul, Korea). For the cell culture, RPMI 1640 (Roswell Park Memorial Institute) medium, DMEM (Dulbecco's modified Eagle's medium), fetal bovine serum (FBS), penicillin−streptomycin, and trypsin ethylenediaminetetraacetic acid (EDTA) were obtained from Gibco (Grand Island, NY). All chemicals were analytical grade and were used without further purification.

Synthesis of Gold Nanorods. Gold nanorods (GNRs) were synthesized in an aqueous CTAB solution using a seed-mediated growth method.[39] The gold seeds were prepared by adding $HAuCl_4$ (0.5 mM, 5 mL) to CTAB (0.2 M, 5 mL), followed by thorough mixing. Then, freshly prepared ice-cold $NaBH_4$ (0.01 M, 600 μL) was added under vigorous stirring, resulting in the formation of a brownish-yellow solution. This solution was stored at room temperature within 1−3 h and was used as the seed solution for the synthesis of gold nanorods. After that, the growth solution was prepared by adding $HAuCl_4$ (1 mM, 5 mL) to the CTAB (0.2 M, 5 mL) solution under thorough stirring. Next, 400 μL of 4 mM $AgNO_3$ (silver nitrate) and 70 μL of 0.0788 M ascorbic acid were added to this solution, which was gently mixed. The color of the mixture (growth solution) changed from yellow to colorless during this process. Then, 12 μL of the seed solution was introduced into the growth solution, was stirred vigorously, and was subsequently kept in a shaking rocker at 100 rpm and 37 °C for about 3 h. The gold nanorod solution showed a light purple color. To remove excess CTAB, the GNR solution was thoroughly purified at least five times by centrifugation at 11 000 rpm for 10 min and was redispersed in deionized water. Finally, the UV−visible absorption spectra of the GNRs were characterized by using a UV spectrophotometer (Agilent 8453, Santa Clara, CA), and the sizes and the aspect ratios of GNRs were measured by using a transmission electron microscopy (TEM; JEM-2100, JEOL, Japan).

Preparation of Pluronic-Based Nanocarriers. Both a bare form (NC(PF 68)) and a chitosan-conjugated form (Chito-NC(PF 68)) of Pluronic-based nanocarriers were prepared by photopolymerizing diacrylated Pluronic (DA-Pluronic) and acrylated chitosan, as previously reported by us.[35,36] In brief, in the case of the bare form, a dilute aqueous solution (2 mL) of diacrylated Pluronic (0.5 wt %) was gently mixed with a photoinitiator (0.05 wt % of Irgacure 2959) and was UV-irradiated for 15 min at a 1.3 mW/cm^2 intensity by using an unfiltered UV lamp (VL-4.LC, 8 W, Vilber Lourmat, France). In the case of the chitosan-conjugated form, a water-soluble glycidyl methacrylate (GMA)-conjugated chitosan (2.8 mg, 0.2 μmol) was dissolved in deionized water and was added into a DA-Pluronic solution (1.5 μmol of DA-PF 68) to make 0.5 wt % of DA-Pluronic. This mixture was photopolymerized at the same condition used for the bare form to allow incorporation of vinyl groups of GMA-conjugated chitosan into the cross-linked nanocarrier. To remove the unreacted substances, the whole solution was dialyzed by using a dialysis bag (cellulose ester, MWCO of 300 kDa) first in 0.1 M NaCl and then in deionized water. After that, the sizes and the surface charges of the nanocarriers were analyzed by using an electrophoretic light scattering spectrophotometer (ELS-Z2, Otsuka Electronics Co., Japan) equipped with a laser diode light source (638 nm) and a photomultiplier tube detector (165° scattering angle). For the chitosan-conjugated form, the amount of chitosan incorporation was 16 wt %, which was determined by using a ninhydrin assay.

Preparation and Characterization of GNR-Loaded Pluronic-Based Nanocarriers. To load the gold nanorods into the Pluronic-based nanocarriers, the GNR solution (50 μg/100 μL) was added into a powdery state of nanocarriers (750 μg) and was incubated at 4 °C for over 12 h, which induced spontaneous loading of the GNRs into the nanocarriers. The encapsulation efficiency (over 90%) and the amount of GNRs loaded inside the nanocarriers were determined by separating the unloaded GNRs at a spin filtration rate at 11 000 rpm for 10 min at room temperature and performing a calculation as reported previously.[49]

Absorption spectra of only GNRs and of the GNR-loaded nanocarriers were measured in the visible to near-infrared light region by using a UV spectrophotometer. The morphologies of the GNRs and the GNR-loaded nanocarriers were observed by using a TEM after a negative staining with a 2% (w/v) phosphotungstic acid solution. The hydrodynamic diameters and surface charges (zeta-potential) of the GNRs and the GNR-loaded nanocarriers in deionized water were analyzed at 37 °C by using an electrophoretic light scattering spectrophotometer (ELS-Z2). The measurements were carried out in triplicate.

***In Vitro* Stability of GNR-Loaded Nanocarriers.** To analyze the optical stability of the GNRs loaded in the nanocarriers, GNRs (as a control group) and the GNR-loaded nanocarrier solution in deionized water (1 mL) were incubated in a shaking rocker at 100 rpm and 37 °C for 1 week and were analyzed by monitoring the UV−vis spectra from 350 to 1000 nm at several time points.

To investigate the stable storage of GNRs inside the nanocarriers, leakage of GNRs from the nanocarriers was characterized. The GNR-loaded nanocarrier solution (100 μL) was placed in a dialysis bag (cellulose ester, MWCO of 300 kDa). The dialysis bag was immersed in 5 mL of phosphate-buffered saline (PBS) containing 10% fetal bovine serum (FBS) in a shaking rocker at 100 rpm and 37 °C. The entire release medium was replaced with the fresh one at each time point to maintain an infinite sink condition. The amount of GNR leakage at each time point was analyzed by using a UV spectrophotometer, and the concentration was calculated from a standard calibration curve. As a control, the release of GNRs from the same setup (dialysis bag) was also analyzed.

***In Vitro* Cytotoxicity Test.** The cytotoxicities of the GNRs and the GNR-loaded nanocarriers were analyzed by using a squamous cell carcinoma (SCC7) tumor cell line and an NIH/3T3 fibroblast cell line. Both types of cells were seeded in 24-well plates at a density of 5 × 10^4 cells per well and were incubated for 24 h at 37 °C. Then, GNRs or GNR-loaded nanocarriers (6.7 wt % loading of GNRs) with concentrations ranging from 1 to 250 μg/mL (based on GNR amount) were added into the plate wells. The cells were further incubated for 2 h at 37 °C. Next, the medium was replaced with 825 μL of fresh medium containing 10-time-diluted WST-1 (Biovision Inc., Mountain View, USA), and the cells were further incubated for 2 h at 37 °C. The absorbance of the colored medium was measured at 450 nm by using a scanning multiwell spectrophotometer (FL600, Bio-Tek, Vermont, USA). The cytotoxicity of the Pluronic-based nanocarriers themselves on SCC7 cells was adapted from a previous report,[36] and the cytotoxicity to the NIH/3T3 fibroblast cells was characterized by using the same protocol.

***In Vitro* Cellular Uptake.** SCC7 or NIH/3T3 fibroblast cells were harvested by using trypsin EDTA and were seeded onto gelatin-coated coverslips (12 mm) in a 24-well tissue culture plate at a density of 5 × 10^4 cells per well and were allowed to grow for 24 h at 37 °C. The coverslips were sterilized in advance by immersion in 70% ethanol and overnight UV exposure and were coated with 2% gelatin for optimal cell growth. The cells were incubated with GNRs or GNR-loaded nanocarriers (50 μg/mL in terms of GNR amount) in the culture medium for 2 h to allow cellular uptake. After incubation, the cells were washed with PBS solution and fixed with 4% formalin solution in PBS for 30 min; the fixed cells were washed with PBS and then with deionized water. The light scattering images were recorded by using a dark-field microscope with a TV lens C-0.45 camera (ECLIPSE L150, Nikon, Tokyo, Japan).

***In Vitro* Photothermal Effect.** SCC7 or NIH/3T3 fibroblast cells were seeded in a 24-well tissue culture plate at a density of 8 × 10^4 cells per well and were allowed to grow for 24 h at 37 °C until being nearly confluent. Then, the medium was replaced with 1 mL of medium containing the GNRs or GNR-loaded nanocarriers (50 μg/mL in terms of GNR amount). After incubation for 2 h, the cells were rinsed three times with PBS buffer to remove the nanomaterials that were nonspecifically adsorbed or remained in the medium. After adding fresh medium, laser light at 780 nm with *ca.* 1.3 mm diameter spot-size and different power densities (41.5 and 26.4 W/cm^2) was irradiated on each well for

4 min by using a CW Ti-sapphire laser (MIRA 900, Coherent Inc., Santa Clara, CA). The cell viability was characterized by using a double staining procedure with acridine orange (AO) and propidium iodide (PI), where green fluorescence from AO indicated live cells and red fluorescence from PI indicated dead cells.[50] Briefly, 1 mL of medium containing 0.67 μM AO and 75 μM PI was added to each well and was incubated in the dark at 37 °C for 30 min. After rinsing with PBS, live and dead cells were visualized by using an inverted fluorescence microscope (TE2000-U, Nikon, Melville, NY).

***In Vivo* Photothermal Therapy.** All animals were obtained from Orient Bio Inc. (Seoul, Korea) and were handled in accordance with the guidelines of the Animal Care and Use Committee of Gwangju Institute of Science and Technology (GIST). To induce a solid tumor, SCC7 cells (1×10^6 in 50 μL PBS) were injected subcutaneously into both the left and the right rear flank areas of male athymic nude mice (CAnN.Cg-Foxn) with ages from 6 to 7 weeks. When the tumors grew to approximately 5 mm in diameter, GNRs or GNR-loaded nanocarriers (100 μg in terms of GNR amount), which were suspended in 0.85% saline solution (100 μL), were intravenously injected through the tail vein; a saline solution was used as a control. First, to investigate the biodistribution of GNRs or GNR-loaded nanocarriers, the mice were sacrificed at 24 h after the i.v. injection. The major organs including tumors were collected and were completely lysed in HNO_3, and then the amounts of GNRs in tissue samples were measured by inductively coupled plasma atomic emission spectrometer (ICP-AES, OPTIMA 4300DV, Perkin-Elmer, California, USA). In addition, to compare the accumulations of nanomaterials in livers and tumors among tissue samples, the excised tissues were fixed in 4% formalin solution for 24 h, and then embedded in optimal cutting temperature (OCT) compound (Tissue-Teks; Sakura Finetek, Kyoto, Japan). For cryostat sectioning, the blocks were frozen at −20 °C and sectioned (5 μm). Then, the tissue sections were stained by using a silver enhancer kit (Sigma-Aldrich Corp., St. Louis, MO) for 10 min according to the manufacturer's instruction. The stained tissue sections were examined by using an inverted fluorescence microscope.

Next, to compare the effect of photothermal ablation of the solid tumors, the mice (left tumors: no laser irradiation *vs* right tumors: laser irradiation) were irradiated with NIR laser light (a 808 nm diode laser, 900 mW, *ca.* 5 mm beam diameter at 4 W/cm^2, Power Technologies, Alexander, AR) for 4 min at 24 h after the i.v. injection of the nanomaterials. The mice were also irradiated with NIR light for 4 min at 24 and 48 h after i.v. injection for the follow-up experiments. Post-treated tumor sizes were measured at given time points by using a digital caliper and were also photographed using a digital camera. All measurements were performed in triplicate. A statistical analysis was performed using the Student *t* test, and for all comparisons, the minimal level of significance was set at $p < 0.05$.

Acknowledgment. This research was partially supported by the National Research Foundation of Korea (NRF) funded MEST of Korea (R15-2008-006-02002-0 and 20100011952), and by the World Class University (WCU) program at GIST through a grant provided by MEST, Korea (R31-2008-000-10026-0).

Supporting Information Available: Figures S1−S4. This material is available free of charge *via* the Internet at http://pubs.acs.org.

REFERENCES AND NOTES

1. Tong, L.; Zhao, Y.; Huff, T. B.; Hansen, M. N.; Wei, A.; Cheng, J. X. Gold Nanorods Mediate Tumor Cell Death by Compromising Membrane Integrity. *Adv. Mater.* **2007,** *19*, 3136–3141.
2. Huang, X.; El-Sayed, I. H.; Qian, W.; El-Sayed, M. A. Cancer Cell Imaging and Photothermal Therapy in the Near-Infrared Region by Using Gold Nanorods. *J. Am. Chem. Soc.* **2006,** *128*, 2115–2120.
3. Chen, C. L.; Kuo, L. R.; Chang, C. L.; Hwu, Y. K.; Huang, C. K.; Lee, S. Y.; Chen, K.; Lin, S. J.; Huang, J. D.; Chen, Y. Y. *In Situ* Real-Time Investigation of Cancer Cell Photothermolysis Mediated by Excited Gold Nanorod Surface Plasmons. *Biomaterials* **2010,** *31*, 4104–4112.
4. von Maltzahn, G.; Centrone, A.; Park, J. H.; Ramanathan, R.; Sailor, M. J.; Hatton, T. A.; Bhatia, S. N. SERS-Coded Gold Nanorods as a Multifunctional Platform for Densely Multiplexed Near-Infrared Imaging and Photothermal Heating. *Adv. Mater.* **2009,** *21*, 3175–3180.
5. Kuo, W. S.; Chang, C. N.; Chang, Y. T.; Yang, M. H.; Chien, Y. H.; Chen, S. J.; Yeh, C. S. Gold Nanorods in Photodynamic Therapy, as Hyperthermia Agents, and in Near-Infrared Optical Imaging. *Angew. Chem., Int. Ed.* **2010,** *49*, 2711–2715.
6. Gobin, A. M.; Lee, M. H.; Halas, N. J.; James, W. D.; Drezek, R. A.; West, J. L. Near-Infrared Resonant Nanoshells for Combined Optical Imaging and Photothermal Cancer Therapy. *Nano Lett.* **2007,** *7*, 1929–1934.
7. Hu, K. W.; Huang, C. C.; Hwu, J. R.; Su, W. C.; Shieh, D. B.; Yeh, C. S. A New Photothermal Therapeutic Agent: Core-Free Nanostructured Au_xAg_{1-x} Dendrites. *Chem.—Eur. J.* **2008,** *14*, 2956–2964.
8. Helmchen, F.; Denk, W. Deep Tissue Two-Photon Microscopy. *Nat. Methods* **2005,** *2*, 932–940.
9. Anderson, R. R.; Parrish, J. A. Selective Photothermolysis: Precise Microsurgery by Selective Absorption of Pulsed Radiation. *Science* **1983,** *220*, 524–527.
10. Chen, W. R.; Adams, R. L.; Carubelli, R.; Nordquist, R. E. Laser-Photosensitizer Assisted Immunotherapy: A Novel Modality for Cancer Treatment. *Cancer Lett.* **1997,** *115*, 25–30.
11. Zharov, V. P.; Galitovskaya, E. N.; Johnson, C.; Kelly, T. Synergistic Enhancement of Selective Nanophotothermolysis with Gold Nanoclusters: Potential for Cancer Therapy. *Lasers Surg. Med.* **2005,** *37*, 219–226.
12. Huang, X.; Jain, P. K.; El-Sayed, I. H.; El-Sayed, M. A. Plasmonic Photothermal Therapy (PPTT) Using Gold Nanoparticles. *Lasers Med. Sci.* **2008,** *23*, 217–228.
13. Hirsch, L. R.; Stafford, R. J.; Bankson, J. A.; Sershen, S. R.; Rivera, B.; Price, R. E.; Hazle, J. D.; Halas, N. J.; West, J. L. Nanoshell-Mediated Near-Infrared Thermal Therapy of Tumors under Magnetic Resonance Guidance. *Proc. Natl. Acad. Sci. U.S.A.* **2003,** *100*, 13549–13554.
14. Loo, C.; Lowery, A.; Halas, N.; West, J.; Drezek, R. Immunotargeted Nanoshells for Integrated Cancer Imaging and Therapy. *Nano Lett.* **2005,** *5*, 709–711.
15. Kim, J.; Park, S.; Lee, J. E.; Jin, S. M.; Lee, J. H.; Lee, I. S.; Yang, I.; Kim, J. S.; Kim, S. K.; Cho, M. H.; *et al.* Designed Fabrication of Multifunctional Magnetic Gold Nanoshells and Their Application to Magnetic Resonance Imaging and Photothermal Therapy. *Angew. Chem., Int. Ed.* **2006,** *45*, 7754–7758.
16. Chen, J.; Wang, D.; Xi, J.; Au, L.; Siekkinen, A.; Warsen, A.; Li, Z. Y.; Zhang, H.; Xia, Y.; Li, X. Immuno Gold Nanocages with Tailored Optical Properties for Targeted Photothermal Destruction of Cancer Cells. *Nano Lett.* **2007,** *7*, 1318–1322.
17. Li, J. L.; Day, D.; Gu, M. Ultra-Low Energy Threshold for Photothermal Therapy of Cancer Using Transferrin-Conjugated Gold Nanorods. *Adv. Mater.* **2008,** *20*, 3866–3871.
18. Sau, T. K.; Murphy, C. J. Seeded High Yield Synthesis of Short Au Nanorods in Aqueous Solution. *Langmuir* **2004,** *20*, 6414–6420.
19. Alkilany, A. M.; Nagaria, P. K.; Hexel, C. R.; Shaw, T. J.; Murphy, C. J.; Wyatt, M. D. Cellular Uptake and Cytotoxicity of Gold Nanorods: Molecular Origin of Cytotoxicity and Surface Effects. *Small* **2009,** *5*, 701–708.
20. Chakravarty, P.; Marches, R.; Zimmerman, N. S.; Swafford, A. D. E.; Bajaj, P.; Musselman, I. H.; Pantano, P.; Draper, R. K.; Vitetta, E. S. Thermal Ablation of Tumor Cells with Antibody-Functionalized Single-Walled Carbon Nanotubes. *Proc. Natl. Acad. Sci. U.S.A.* **2008,** *105*, 8697–8702.
21. Li, Y.; Lu, W.; Huang, Q.; Huang, M.; Li, C.; Chen, W. Copper Sulfide Nanoparticles for Photothermal Ablation of Tumor Cells. *Nanomedicine* **2010,** *5*, 1161–1171.
22. Zhou, W.; Shao, J.; Jin, Q.; Wei, Q.; Tang, J.; Ji, J. Zwitterionic Phosphorylcholine as a Better Ligand for Gold Nanorods Cell Uptake and Selective Photothermal Ablation of Cancer Cells. *Chem. Commun.* **2010,** *46*, 1479–1481.

23. Huang, H. C.; Barua, S.; Kay, D. B.; Rege, K. Simultaneous Enhancement of Photothermal Stability and Gene Delivery Efficacy of Gold Nanorods Using Polyelectrolytes. *ACS Nano* **2009,** *3*, 2941–2952.
24. Connor, E. E.; Mwamuka, J.; Gole, A.; Murphy, C. J.; Wyatt, M. D. Gold Nanoparticles Are Taken up by Human Cells but Do Not Cause Acute Cytotoxicity. *Small* **2005,** *1*, 325–327.
25. Huang, X.; Neretina, S.; El-Sayed, M. A. Gold Nanorods: From Synthesis and Properties to Biological and Biomedical Applications. *Adv. Mater.* **2009,** *21*, 4880–4910.
26. Takahashi, H.; Niidome, Y.; Niidome, T.; Kaneko, K.; Kawasaki, H.; Yamada, S. Modification of Gold Nanorods Using Phosphatidylcholine To Reduce Cytotoxicity. *Langmuir* **2006,** *22*, 2–5.
27. Hauck, T. S.; Ghazani, A. A.; Chan, W. C. Assessing the Effect of Surface Chemistry on Gold Nanorod Uptake, Toxicity, and Gene Expression in Mammalian Cells. *Small* **2008,** *4*, 153–159.
28. Kim, E.; Yang, J.; Choi, J.; Suh, J. S.; Huh, Y. M.; Haam, S. Synthesis of Gold Nanorod-Embedded Polymeric Nanoparticles by a Nanoprecipitation Method for Use as Photothermal Agents. *Nanotechnology* **2009,** *20*, 365602.
29. Niidome, T.; Akiyama, Y.; Yamagata, M.; Kawano, T.; Mori, T.; Niidome, Y.; Katayama, Y. Poly(ethylene glycol)-Modified Gold Nanorods as a Photothermal Nanodevice for Hyperthermia. *J. Biomater. Sci. Polym. Ed.* **2009,** *20*, 1203–1215.
30. von Maltzahn, G.; Park, J. H.; Agrawal, A.; Bandaru, N. K.; Das, S. K.; Sailor, M. J.; Bhatia, S. N. Computationally Guided Photothermal Tumor Therapy Using Long-Circulating Gold Nanorod Antennas. *Cancer Res.* **2009,** *69*, 3892–3900.
31. Huang, Y. F.; Sefah, K.; Bamrungsap, S.; Chang, H. T.; Tan, W. Selective Photothermal Therapy for Mixed Cancer Cells Using Aptamer-Conjugated Nanorods. *Langmuir* **2008,** *24*, 11860–11865.
32. Huff, T. B.; Tong, L.; Zhao, Y.; Hansen, M. N.; Cheng, J. X.; Wei, A. Hyperthermic Effects of Gold Nanorods on Tumor Cells. *Nanomedicine* **2007,** *2*, 125–132.
33. Li, Z.; Huang, P.; Zhang, X.; Lin, J.; Yang, S.; Liu, B.; Gao, F.; Xi, P.; Ren, Q.; Cui, D. RGD-Conjugated Dendrimer-Modified Gold Nanorods for *In Vivo* Tumor Targeting and Photothermal Therapy. *Mol. Pharmaceutics* **2010,** *7*, 94–104.
34. Dickerson, E. B.; Dreaden, E. C.; Huang, X.; El-Sayed, I. H.; Chu, H.; Pushpanketh, S.; McDonald, J. F.; El-Sayed, M. A. Gold Nanorod Assisted Near-Infrared Plasmonic Photothermal Therapy (PPTT) of Squamous Cell Carcinoma in Mice. *Cancer Lett.* **2008,** *269*, 57–66.
35. Choi, W. I.; Tae, G.; Kim, Y. H. One Pot, Single Phase Synthesis of Thermo-Sensitive Nano-Carriers by Photo-Crosslinking of a Diacrylated Pluronic. *J. Mater. Chem.* **2008,** *18*, 2769–2774.
36. Kim, J.-Y.; Choi, W. I.; Kim, Y. H.; Tae, G.; Lee, S. Y.; Kim, K.; Kwon, I. C. *In-Vivo* Tumor Targeting of Pluronic-Based Nano-Carriers. *J. Controlled Release* **2010,** *147*, 109–117.
37. Jain, P. K.; Lee, K. S.; El-Sayed, I. H.; El-Sayed, M. A. Calculated Absorption and Scattering Properties of Gold Nanoparticles of Different Size, Shape, and Composition: Applications in Biological Imaging and Biomedicine. *J. Phys. Chem. B* **2006,** *110*, 7238–7248.
38. Kumar, S.; Harrison, N.; Richards-Kortum, R.; Sokolov, K. Plasmonic Nanosensors for Imaging Intracellular Biomarkers in Live Cells. *Nano Lett.* **2007,** *7*, 1338–1343.
39. Nikoobakht, B.; El-Sayed, M. A. Preparation and Growth Mechanism of Gold Nanorods (NRs) Using Seed-Mediated Growth Method. *Chem. Mater.* **2003,** *15*, 1957–1962.
40. Iqbal, M.; Tae, G. Unstable Reshaping of Gold Nanorods Prepared by a Wet Chemical Method in the Presence of Silver Nitrate. *J. Nanosci. Nanotechnol.* **2006,** *6*, 3355–3359.
41. Iqbal, M.; Chung, Y.-I.; Tae, G. An Enhanced Synthesis of Gold Nanorods by the Addition of Pluronic (F-127) *via* a Seed Mediated Growth Process. *J. Mater. Chem.* **2007,** *4*, 335–342.
42. Chung, Y. I.; Kim, J. C.; Kim, Y. H.; Tae, G.; Lee, S. Y.; Kim, K.; Kwon, I. C. The Effect of Surface Functionalization of PLGA Nanoparticles by Heparin- or Chitosan-Conjugated Pluronic on Tumor Targeting. *J. Controlled Release* **2010,** *143*, 374–382.
43. Yang, R.; Shim, W. S.; Cui, F. D.; Cheng, G.; Han, X.; Jin, Q. R.; Kim, D. D.; Chung, S. J.; Shim, C. K. Enhanced Electrostatic Interaction between Chitosan-Modified PLGA Nanoparticle and Tumor. *Int. J. Pharm.* **2009,** *371*, 142–147.
44. Nam, H. Y.; Kwon, S. M.; Chung, H.; Lee, S. Y.; Kwon, S. H.; Jeon, H.; Kim, Y.; Park, J. H.; Kim, J.; Her, S.; *et al.* Cellular Uptake Mechanism and Intracellular Fate of Hydrophobically Modified Glycol Chitosan Nanoparticles. *J. Controlled Release* **2009,** *135*, 259–267.
45. Park, S.; Lee, S. J.; Chung, H.; Her, S.; Choi, Y.; Kim, K.; Choi, K.; Kwon, I. C. Cellular Uptake Pathway and Drug Release Characteristics of Drug-Encapsulated Glycol Chitosan Nanoparticles in Live Cells. *Microsc. Res. Tech.* **2010,** *73*, 857–865.
46. Pan, Y.; Neuss, S.; Leifert, A.; Fischler, M.; Wen, F.; Simon, U.; Schmid, G.; Brandau, W.; Jahnen-Dechent, W. Size-Dependent Cytotoxicity of Gold Nanoparticles. *Small* **2007,** *3*, 1941–1949.
47. Pissuwan, D.; Valenzuela, S. M.; Miller, C. M.; Cortie, M. B. A Golden Bullet? Selective Targeting of Toxoplasma Gondii Tachyzoites Using Antibody-Functionalized Gold Nanorods. *Nano Lett.* **2007,** *7*, 3808–3812.
48. Niidome, T.; Yamagata, M.; Okamoto, Y.; Akiyama, Y.; Takahashi, H.; Kawano, T.; Katayama, Y.; Niidome, Y. PEG-Modified Gold Nanorods with a Stealth Character for *In Vivo* Applications. *J. Controlled Release* **2006,** *114*, 343–347.
49. Li, F. Q.; Su, H.; Wang, J.; Liu, J. Y.; Zhu, Q. G.; Fei, Y. B.; Pan, Y. H.; Hu, J. H. Preparation and Characterization of Sodium Ferulate Entrapped Bovine Serum Albumin Nanoparticles for Liver Targeting. *Int. J. Pharm.* **2008,** *349*, 274–282.
50. Tae, G.; Kim, Y. J.; Choi, W. I.; Kim, M.; Stayton, P. S.; Hoffman, A. S. Formation of a Novel Heparin-Based Hydrogel in the Presence of Heparin-Binding Biomolecules. *Biomacromolecules* **2007,** *8*, 1979–1986.